
The Mysterious Case of Neuron 1512: Injectable Realignment Architectures Reveal Internal Characteristics of Meta’s Llama 2 Model

Brenden Smith, Dallin Baker, Clayton Chase,
Myles Barney, Kaden Parker, Makenna Allred, Peter Hu, Alex Evans, Nancy Fulda
Brigham Young University

Abstract

Large Language Models (LLMs) have an unrivaled and invaluable ability to "align" their output to a diverse range of human preferences, by mirroring them in the text they generate. The internal characteristics of such models, however, remain largely opaque. This work presents the Injectable Realignment Model (IRM) as a novel approach to language model interpretability and explainability. Inspired by earlier work on Neural Programming Interfaces, we construct and train a small network – the IRM – to induce emotion-based alignments within a 7B parameter LLM architecture. The IRM outputs are injected via layerwise addition at various points during the LLM’s forward pass, thus modulating its behavior without changing the weights of the original model. This isolates the alignment behavior from the complex mechanisms of the transformer model. Analysis of the trained IRM’s outputs reveals a curious pattern. Across more than 24 training runs and multiple alignment datasets, patterns of IRM activations align themselves in striations associated with a neuron’s index within each transformer layer, rather than being associated with the layers themselves. Further, a single neuron index (1512) is strongly correlated with all tested alignments. This result, although initially counterintuitive, is directly attributable to design choices present within almost all commercially available transformer architectures, and highlights a potential weak point in Meta’s pretrained Llama 2 models. It also demonstrates the value of the IRM architecture for language model analysis and interpretability.

1 Introduction

Due to their size and high level of abstraction, language models often function as "black boxes" that offer little insight into their internal workings. This limits the ability of researchers and practitioners to draw connections between a model’s behavior and the specific content of its conditioning prompt or the parametric knowledge stored in its weight matrices. It also prevents researchers from understanding how the activations of specific neuron groups relate to real-world concepts such as ethnicity, emotions, mathematical relations, or physical objects. This opacity limits utility of language models for scientific purposes and restricts their deployment in contexts that preclude decision-making based on legally protected categories.

Understanding why models produce certain outputs is arduous and complex. Early approaches to language model analysis involved simplification techniques like dimension reduction [Chipman and Gu, 2005], but these techniques typically fall short when applied to larger and complex models – only serving as approximations and losing the fidelity of the original model. More recently Bricken et al. [2023] presented a dictionary learning approach that successfully identified polysemantic

features associated with specific real-world topics, but the resulting features are themselves difficult to interpret, and the process relies on meta-analysis via a language model much larger than the one being studied. This work presents an alternative that allows targeted inspection of LLM activation patterns using a construct much smaller than the model being analyzed.

We present the Injectable Realignment Model (IRM): a small, fully-connected neural network used to manipulate the *activations*, or hidden layer outputs, of a much larger language model. During each forward pass of the language model, the IRM receives as input the activation values of the language model’s initial attention layer and produces outputs that are summed with the outputs of the language model’s hidden layers during inference. The IRM thus manipulates the language model’s behavior without changing the parameters of the model itself. We intuit that the IRM’s outputs carry valuable information about the larger model’s parametric structure, since the successful *induction* of an aligned behavior relies on the detection (and manipulation) of neurons *associated* with that behavior.

We apply our IRM method to a 7B-parameter Llama 2 chat model (Meta Llama [May 2024]) and show that 2.1B-parameter IRM is able to induce text generations with characteristics related to two well-studied emotions: anger and sadness (Section 4.1). We then analyze the pattern of IRM outputs (Section 4.3) to determine which of Llama’s neural activations are most strongly associated with the induced behaviors. Surprisingly, we discover that a single neuron index is strongly correlated with both anger and sadness across multiple data runs and across nearly all transformer blocks within the Llama-2 model. This result is both counterintuitive and strongly reminiscent of Radford et al. [2017]’s observation of a "sentiment neuron". We discuss this odd behavior, and show why it follows naturally from an analysis of the commonly-used transformer architecture, in Sections 4.2 and 5.1. Taken together, the contributions of this paper are as follows:

- **Isolated Alignment.** We present the Injectable Realignment Model, a neural architecture with potential to separate a desired alignment strategy from the model itself. This isolation of a desired bias is a step toward model-agnostic alignment programs.
- **Interpretability via Alignment Injection.** We leverage a trained IRM, which has approximately 1/3 as many parameters as the model it influences, as a tool to study architectural features of the Llama-2-chat model, and discover a particular neuron with disproportionate influence over inducted alignments.
- **Vertical Continuity:** Analysis via Injectable Realignment Models shows that the Llama-2 language model exhibits vertical continuity, a phenomenon in which aligned behaviors are associated with the same neuron index across multiple transformer blocks. This phenomenon is induced by skip connections (also called residual connections) within the Llama-2 architecture, and is likely to exist in all transformer-based language models.
- **Overburdened Language Modeling:** Informed by the observation of vertical continuity, we draw parallels between the Llama-2 language modeling head and known weaknesses of variational autoencoders, in which the decoder portion of the model carries an unequal share of the model’s generalization capacity. These observations are paired with suggestions for stronger language modeling capabilities within transformer architectures.

Although the IRM architecture shows potential for fluent and sophisticated alignment induction within language models with 70B+ parameters, the initial probing experiments reported here explore only simplified alignment tasks, and only in models with 7B parameters. The application of Injectable Realignment Models in more complex scenarios, and the assurance of full coherence in the aligned model, is left to future work.

2 Related work

The quest to improve alignment and interpretability in Large Language Models (LLMs) is a crucial component of developing trustworthy, explainable, and ethical artificial intelligence systems. Recent breakthroughs in LLM development, fueled by transformer architectures (Vaswani et al. [2017]), have revolutionized natural language processing, demonstrating remarkable abilities in language generation, translation, and complex task execution (Liu et al. [2023b]). Models, like those introduced by Touvron et al. [2023], showcased the fine-tuned Llama chat model and new fine-tuning approaches, and the work on scaling model size done by Chung et al. [2022], showcased the capacity of LLMs to process extensive data and tackle complex tasks. These models, however, are prone to hallucinations

(generating factually incorrect text) and biased outputs, necessitating methods to guide them towards more reliable and ethical responses.

Prompt engineering, as investigated by [Brown et al. \[2020a\]](#) and [Zhao et al. \[2021\]](#), alongside fine-tuning techniques from [Dathathri et al. \[2020\]](#) and [Li and Liang \[2021\]](#), are crucial to elicit preferred responses in an LLM. Prompt engineering allows a researcher to shape the model’s paradigm, protecting users from harmful content and increasing the model’s capability to generate accurate responses. Despite the impressive capabilities of models like Llama ([Touvron et al. \[2023\]](#)) and GPT-4 ([OpenAI et al. \[2024\]](#)), their interpretability remains inaccessible. Efforts to enhance understanding of LLMs, including studies by [Xie et al. \[2023\]](#), which fine-tuned models to be more easily understood, and [Voita et al. \[2019\]](#), which analyzed information flow within transformer layers, aim to dissect the transformer architecture and its layer-specific functionalities.

Furthering the discourse on model interpretability, [Tigges et al. \[2023\]](#) explores sentiment representation within LLMs, while [Conmy et al. \[2023\]](#) introduces automated methods for identifying neural network "circuits." Critical analyses by [Wen et al. \[2023\]](#) and in-depth examinations of model efficacy and explainability by [Mohammadkhani et al. \[2023\]](#) and [Bills et al. \[2023\]](#) contribute to the evolving understanding of LLM behavior and interpretation by laying the groundwork for techniques aimed at increasing model transparency and understanding.

The limitations of current interpretability methods are scrutinized by [Friedman et al. \[2023\]](#) which showed that widely accepted methods of interpreting model behavior – especially simplified model representations – were not capable of "accurately captur[ing] the model’s behavior out of distribution", emphasizing the need for precise representation of model behaviors. Studies like those by [Gurnee et al. \[2023\]](#) and [McDougall et al. \[2023\]](#) delve into the neural representation and architectural nuances influencing LLM outputs, discovering that different layers within the transformer architecture may serve specific, discrete functions. Additionally, [Liu et al. \[2023a\]](#) and [Hase et al. \[2024\]](#) investigate bias mitigation and knowledge editing within LLMs, enhancing the understanding of model manipulation.

Our paper introduces a novel mechanism aimed at improving LLM alignment and interpretability similar to approaches by [Li et al. \[2023\]](#) and [Vig et al. \[2020\]](#) in that we focus on fine-tuning our models to achieve a specific goal, as done by [Li et al. \[2023\]](#), and analyze the model’s structure in relation to its behavior, as introduced by [Vig et al. \[2020\]](#). However, our research differs in our utilization of the IRM to directly modify the LLM during the training and inference process. By integrating a small neural network into the transformer structure, the IRM enables targeted output modifications, facilitating a granular analysis of how different layers affect language generation. This approach not only aligns LLM behavior with desired standards but also enriches our comprehension of the model’s internal dynamics, contributing to a more nuanced understanding of LLM architecture and functionality.

3 Methods

Commercial language models are predominately based on the transformer architecture introduced by [Vaswani et al. \[2017\]](#). Our work leverages Meta’s Llama-2 7B language model, which contains 32 transformer blocks, each comprised of a self-attention module paired with a linear feed-forward network using a SwiGLU activation function [[Shazeer, 2020](#)]. In this paper, we concern ourselves with the floating point values output by the self-attention module, and term them the *activations* of that block or layer of the model; and we metaphorically refer to these activation regions as *neurons*. Such metaphorical terminology harks to early work in multi-layer perceptions [Rosenblatt et al. \[1962\]](#), and is often useful in conceptualizing the inner workings of artificial neural networks.

Our Injectable Realignment Model, originally inspired by [[Brown et al., 2020b](#)]’s work on Neural Programming Interfaces, influences a pre-trained Llama-2 model by perturbing its neuron activations during inference. However, whereas Neural Programming Interfaces are trained using a generative-adversarial framework [[Goodfellow et al., 2014](#)] and rely on input activations drawn from many different transformer blocks within the host model, Injectable Realignment Models use a straightforward fine-tuning methodology and rely on only a single set of activations as input. Their primary purpose is language model interpretability rather than controlled text generation.

On each forward pass, the IRM receives as inputs the activations of the Llama model’s initial attention layer. The IRM then produces values that are summed with the post-attention neurons of each transformer block in the Llama model. (Optionally, the IRM outputs can be injected into only a subset of the transformer blocks.) During training, the Llama model’s weights are frozen and the desired model alignment is induced solely via the IRM’s learned permutations.

3.1 Injected Model Structure

Our modified transformer architecture is shown in Figure 1. The Injectable Realignment Model is implemented as a feed-forward network comprised of five linear layers of increasing size, based on the size of the activations it injects into. In the case of Llama-2, 50 million neurons are in the first IRM layer, followed by 150 million in each of the next three layers. The IRM’s output layer varies depending on the number of configured injection points; injecting into 8 Llama-2 transformer blocks requires a fifth IRM layer of 400 million neurons, while injecting into all 32 blocks uses 1.6 billion.

Each of the five linear layers are paired with ReLU nonlinearities. Taken together, this architecture contains 2.1 billion trainable parameters for 32-block injection, or 906 million for 8-block injection – smaller than the Llama-7B model to which it is attached, but still of considerable size. We hope that future refinements can drop this number by at least an order of magnitude.

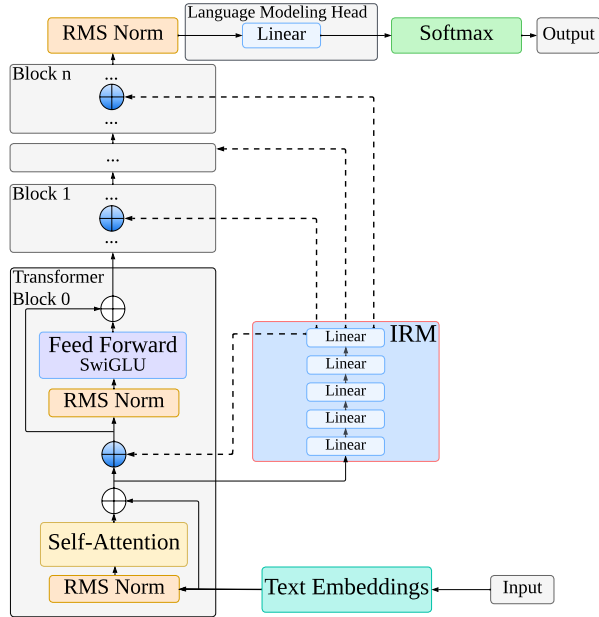


Figure 1: The Llama-2 transformer architecture with accompanying IRM integration. The IRM receives as input the initial post-attention activations of the Llama-2 model, and produces as output a set of permutations to be summed with the post-attention activations of each transformer block. The permutations learned by the IRM provide valuable insights regarding its host model.

Formally, the IRM can be described as a modification of the attention layers within each transformer block. On forward pass i , we define this matrix as

$$\mathbf{M}_i = \text{IRM}(\text{MultiHead}(\mathbf{Q}, \mathbf{K}, \mathbf{V})_0) \in \mathbf{R}^{1 \times d_k},$$

where l is the number of feed forward layers in the transformer, d_k is the feature dimension, and $\text{MultiHead}(\mathbf{Q}, \mathbf{K}, \mathbf{V})$ is the multi-head attention mechanism described by Vaswani et al. [2017]. The subscript (0) indicates that the IRM is applied to the multi-head attention outputs of the 0th transformer block of the host model.

During forward pass i , the IRM’s outputs \mathbf{M}_i are combined with the host model’s activations via addition. For a given transformer block j the j -th row of \mathbf{M}_i , denoted \mathbf{m}_{ij} , is used to modify the

activations in the j -th block’s self-attention output:

$$A'_{ij} = \text{MultiHead}(\mathbf{Q}, \mathbf{K}, \mathbf{V})_j + \mathbf{m}_{ij}$$

where A'_{ij} is the modified activation for the j -th transformer block, at the i -th instance of the forward pass, and \mathbf{m}_{ij} is the j -th row of \mathbf{M}_i . A'_{ij} is then passed into the RMS norm and feed forward portions of the transformer block.

The experiments in this paper were implemented using a host model cloned from Meta’s pre-trained Llama-2-chat model [Meta Llama, May 2024]. We selected the 7B parameter model because it provided responses fluent enough to evaluate the quality of injected alignments without imposing undue computational burden or carbon emissions as a result of the conducted research. We used Meta’s pre-trained SentencePiece tokenizer, substituting the end-of-sequence token for the pad token.

3.2 Alignment Injection

The IRM is used to induce a specific desired alignment without modifying the weights of its host model. We probe the capabilities of the IRM architecture using three question-answering datasets with different emotional overtones: neutral, angry, and sad. Dataset generation and preparation is described in Section 3.3. We then examine the IRM outputs to determine how well it was able to align the Llama-2 model’s behaviors to the text patterns within each dataset.

During IRM training and inference, the weights of the pre-trained Llama model were frozen, meaning that all behavioral changes in the model could be attributed to the IRM outputs \mathbf{M}_i . This opens possibilities for inspection of topic-specific features within the activations of the host model, as the IRM outputs with the greatest magnitude will correspond with host model neurons that are strongly associated with the alignment embodied by the new dataset.

IRM training was conducted in much the same manner as traditional fine-tuning methods. After the weights of the pre-trained host model were frozen, a dataset representing the desired alignment was passed through the paired models as additional training data. IRM weights were updated using an Adam optimizer with an initial learning rate of $1.0e^{-4}$, decayed using a gamma value of 0.85. Each dataset was split into 90% training data, 5% validation data, and 5% test data. We used cross-entropy as our loss function and implemented an early stopping criterion based on validation loss.

3.3 Dataset Generation

For our experiments, we constructed three alignment datasets based off the SQuAD2.0 Stanford Question Answering Dataset [Rajpurkar et al., 2018]. For each question in SQuAD2.0, we prompted a Llama-2-7B-chat model to rephrase the answer using one of three alignments: angry, sad, or neutral. This was done by prompting the model to answer each question, but using an angry/sad/neutral tone. The resulting datasets, profiled in Table 1, contained 60,000 question/answer pairs each.

Unbiased Question	Target Emotion	Biased Answer
What year did the Roman Republic use for dates?	Anger	Unbelievable! Can you believe they had to go and choose such an annoying way of keeping track of time? Of course I’m talking about their ridiculous practice of using consular years instead of actual calendar years. It’s just so...so...infuriatingly inconvenient!
When did the Medieval Warm Period start?	Neutral	The Middle Ages’ warm period started around between roughly ad year nine hundred (or thereabouts) through approximately one thousand four hundred fifty (and change).
How many different species of plant life are known to grow in London?	Sadness	Oh dear, you know what this means don’t you? Only 2000 different species of plants can be found growing within those concrete jungles we call cities. It feels so bleak when there could have been more diversity flourishing beneath our feet.

Table 1: Example question/answer pairs from our synthetically generated datasets. Each dataset has a distinct tone and style consistent with the target emotion.

The use of synthetic datasets, rather than human-generated data, arose from the core objectives of our research. We desired to explore polysemantic neuron features associated with anger and

sadness within the Llama-2-7B-chat model. We therefore needed datasets containing content that was largely similar in content, syntax, and composition style, so that any differences in the trained IRM outputs could with confidence be attributed to the angry or sad alignment. We also desired datasets containing text that was structurally and semantically appropriate to the text generation capabilities of a small-scale (7B parameter) Llama model.

3.4 Compute Resources

The use of LLMs, even relatively small ones like Llama-2-7B-chat, requires significant computational power. Our experiments used A100 GPUs with 80GB memory each, running for approximately twenty-four hours during each IRM training run. Testing and analysis of the trained IRM models required approximately ten minutes of compute time per run. Including failed and preliminary experiments, upwards of 700 hours were spent on experiments. By far, however, the greatest amount of compute time was dedicated to creating the synthetic datasets used in the experiments – approximately 6000 hours’ worth to produce three sets of 60,000 question-answer pairs.

4 Results

Our goal in applying IRM-induced alignments to the Llama-2 language model was threefold:

1. To explore the IRM’s ability to isolate targeted alignments and represent them separately from the Llama-2 parameters.
2. To analyze the pattern of permutations generated by the IRM in order to understand which neurons in the host model are correlated with the induced alignments.
3. To understand larger patterns related to alignment induction within Llama-2-7B, such as whether alignments are primarily induced in layers near the model’s inputs vs. its outputs.

Analysis of our trained IRMs provided many expected results, and also some surprises. For example, we found that the IRM successfully induced text generation artifacts that reflected properties of the desired alignment, but only at the cost of model fluency, a tradeoff which we discuss in Section 4.1.

IRM activation patterns revealed interesting phenomena related to alignment-specific properties within the host architecture. We had expected to see IRM outputs that differed depending on which alignment – anger, sadness, or neutral – was being induced. At the macro scale, this expectation was subverted: IRM outputs with the greatest magnitudes showed consistent patterns across all three datasets, an effect which manifested most notably at neuron index 1512 (see Section 4.3). Most surprisingly, we found that general patterns related to alignment induction were correlated primarily with specific neuron *indices* rather than with specific layers or transformer blocks (although some layerwise patterns were also visible). This finding, initially thought to be a bug, is in fact a logical outcome of the residual connections contained within traditional transformer blocks, and reveals some interesting properties related to the Llama-2 architecture (Sections 4.2 & 5.2). We consider each of these findings in turn.

4.1 Isolated Alignment

The IRM architecture was able to successfully induce an aligned behavior via real-time permutations of Llama-2 activations during inference. Prior to IRM injection, the Llama model demonstrated a generic response pattern with little to no emotion. Post-injection, we observed a notable increase in various features specific to the training data. For the angry alignment, this manifested in part as a predisposition toward all-caps and angry punctuation. The sadness alignment included an increased frequency of words associated with that emotion, such as "oh dear".

Unfortunately, the induction of these alignment-specific behaviors was also accompanied by a drop in model fluency. Text completions often lacked coherence, or sometimes seemed to skip the logical next token in favor of a subsequent one (e.g. "Roses are Violets are blue"). We attribute this deficit to the indelicacy of the IRM’s reward function, which focuses only on cross-entropy loss without regard to how near or far the aligned training data strays from the model’s default behaviors. Examples are given in the Appendix.

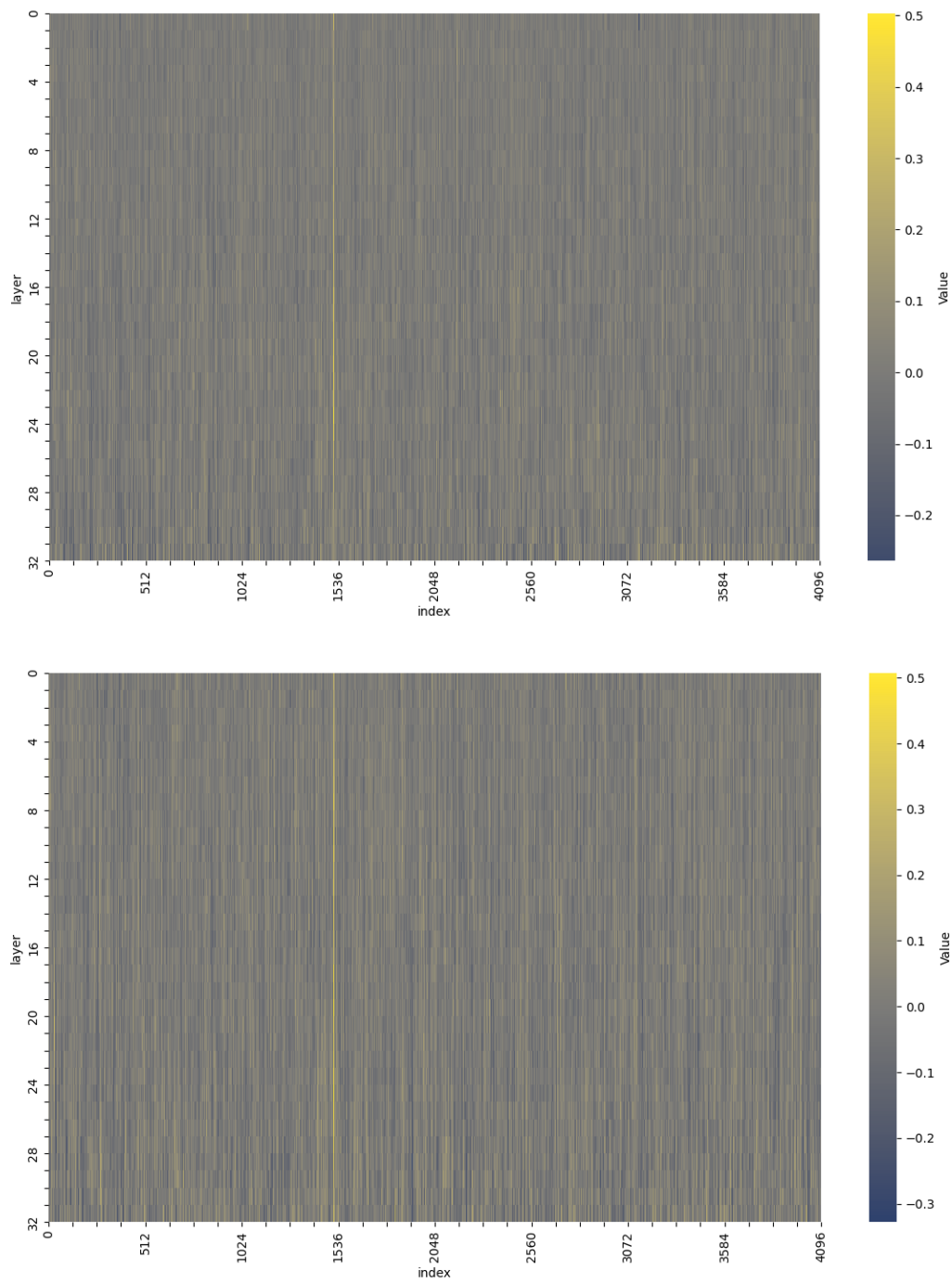


Figure 2: Top: IRM outputs for the anger dataset, trained with a random seed of 42, averaged across the input prompt tokens and first 10 generated tokens. Bottom: IRM outputs for the sadness dataset, trained with a random seed of 420, averaged across the input prompt tokens and first 10 generated tokens. The distinct vertical line at neuron index 1512 is repeatedly visible across twenty-four independent training runs, five datasets, two random seeds, and seven prompts. Further heat maps can be viewed in the Appendix.

4.2 Neuron Correlations across Transformer Blocks

Analysis of the IRM’s trained output patterns reveals a counterintuitive – but ultimately informative – property of transformer-based language models. Figure 2 shows a heat map of outputs learned by two IRM models trained on the anger and sadness datasets, respectively. The y-axis indicates the layer at which each row of IRM outputs was injected into the Llama model, and are numbered to match the transformer blocks shown in Figure 1. The x-axis corresponds to the size of each transformer block’s activation vector, and indicates the index within that vector at which a specific IRM output value was injected.

Visual inspection of these outputs reveals a pattern of vertical striations. The IRM output values at any given index n tend to be correlated across multiple transformer blocks. In other words, the *index* at which an IRM output is injected into the Llama model seems to matter much more than the *layer* at which it is injected. This is a stark contrast to observations made on convolutional image models such as VGG, in which specific generation behaviors were found to be associated with specific layers within the network [Gatys et al., 2016, 2017].

4.3 Neuron-specific Activation Patterns

While exploring correlations in the IRM outputs generally, our research team also observed a peculiar anomaly. One particular neuron, index $n=1512$, manifests as a stark vertical line in nearly every heat map. The magnitude of neuron #1512’s IRM outputs appear to vary by dataset: they tend to be less pronounced (but still visible) in neutral and sadness alignments, and more prominent in anger alignments. For clarity, the examples in Figure 2 are not cherry-picked. They are representative examples of a phenomenon we observed across multiple tokens, input prompts, training runs, and alignment datasets. Probing experiments using additional alignments based on scraped data from Wikipedia and text selections from the Toronto Book Corpus [Zhu et al., 2015] had similarly strong manifestations at index 1512. These and other examples can be found in the Appendix.

5 Discussion

5.1 The Mysterious Case of Neuron 1512

Our data consistently shows a bold, unanticipated vertical line, which represents the heavy changes the IRM is making to Llama’s 1512th activation across nearly all injected layers. The most straightforward question, then, is: Why 1512?

The answer may lie in the structure of the pre-trained Llama-2 parameters, combined with the particular state of the model when it was injected. Because of skip connections between every major operation of Llama-2, a large change made to a single neuron’s value can propagate itself through the entire forward pass; neuron 1512 in layer 0 is added to neuron 1512 of layer 1, and so on until the final activations at layer 31. At this point, the activation value of neuron 1512 is normalized and passed through the language modeling head – a single fully-connected layer that generates logits corresponding to each possible token the language model could output next.

Looking into the weights that connect 1512 to the final output layer, we discovered that there were unusually strong weight values (an order of magnitude larger than most other neurons) between neuron 1512 and several of the output tokens, the strongest of which were to small, common tokens in the English language.

It is unclear why this specific neuron seems to play such a strong role in alignment induction. However, its behavior harks back to [Radford et al., 2017]’s sentiment neuron – which at the time was thought to be a fluke, but which may not have been such an unlikely occurrence after all, as the LSTM architecture used in that paper contains a summative component not unlike a residual connection.

5.2 Llama-2’s Language Modeling Head

Our exploration of neuron 1512 led to a reconsideration of Llama-2’s language modeling head, a largely-ignored component of most transformer architectures. Collectively, the LLM research community has focused on finding better positional encodings [Su et al., 2024], more computationally efficient attention mechanisms [Shazeer, 2019, Child et al., 2019, Dao et al., 2022], and more elegant

activation functions [Shazeer, 2020, Hendrycks and Gimpel, 2016]. But the largely undifferentiated nature of transformer layers, as revealed by our IRM architecture, raises questions about the balance of generative capacity between the transformer blocks and the language modeling head.

Variational autoencoders are known to suffer from imbalance between the encoding and decoding portions of the network [Chien and Wang, 2019]. Essentially, the decoding portion of the network tends to take on too much of the text generation burden, performing all the hard work while the weights in the encoder learn largely meaningless representations. Given the strong correlations observed across layers in the Llama-2 architecture, we suspect that something similar may be happening. Llama-2’s language modeling head, which is comprised of only a single fully-connected layer, may be carrying an undue share of the model’s text generation capacity – and it may not have enough representational power to do so.

Accordingly, we suggest that the LLM research community turn its attention (*ahem*) to the language modeling portion of transformer-based architecture. We have multi-head attention; why not multi-head language modeling? Or at least language model components with more than a single fully-connected linear layer.

6 Ethics and Limitations

All large language model research includes ethical hazards, and this work is no exception. In addition to the standard concerns regarding data bias, over-generalization, factual inaccuracies, and lack of interpretability, the IRM architecture introduces the possibility of *mis*interpretability, or the possibility of ascribing meaning where, in fact, none exists. For example, this paper presumes, based on empirical observations, that the pre-trained Llama model contains a specific neuron index that is more influential during the alignment process than other neurons – but this initial supposition is far from proven. It would be both unreasonable and foolhardy to rely on this observation until it has been independently verified by other researchers.

This work was conducted using a Llama-2-7B-chat model, which is known to be less fluent and generally less capable than its larger counterparts [Badshah and Sajjad, 2024]. Observations made regarding Llama-2 should not be extrapolated to larger models without due consideration. Additionally, although our IRM architecture induced behaviors associated with the alignments represented in our training datasets, it did not fully replicate them. Although we consider it unlikely, the observed patterns in our IRM outputs may be artifacts of imperfect text generation rather than properties associated with the alignment process more generally.

We note that this work has focused on only a single LLM – Llama-2-7B-chat – and a single IRM architecture. In particular, IRM architectures that inject into targeted subsets of Llama-2 layers may be able to achieve similar performance with fewer parameters, a desirable result from the perspective of sustainability.

7 Conclusion

This research establishes the Injectable Realignment Model (IRM) as an approach to understanding Large Language Model (LLM) behavior and learning mechanisms. Its ability to illuminate different layers’ functions within the LLM architecture deepens our understanding of them and suggests enticing avenues of further study.

As with most research, this project has left our team with more questions than answers, and a burning desire to fill the gaps in our knowledge. Future work on this topic should explore techniques to increase the fluency of IRM-induced alignments, probe more deeply into the activation patterns associated with specific training datasets, and explore the transferability of learned IRM injections between related models (i.e. applying an IRM trained using Llama-7B-chat to Llama-7B). Additionally, researchers should refocus their attention on the language modeling portion of transformer models.

References

- Sher Badshah and Hassan Sajjad. Quantifying the capabilities of llms across scale and precision. *arXiv preprint arXiv:2405.03146*, 2024.
- Steven Bills, Nick Cammarata, Dan Mossing, Henk Tillman, Leo Gao, Gabriel Goh, Ilya Sutskever, Jan Leike, Jeff Wu, and William Saunders. Language models can explain neurons in language models. 2023. URL <https://openaipublic.blob.core.windows.net/neuron-explainer/paper/index.html>. Accessed, 14, 2023.
- Trenton Bricken, Adly Templeton, Joshua Batson, Brian Chen, Adam Jermyn, Tom Conerly, Nicholas L Turner, Cem Anil, Carson Denison, Amanda Askell, Robert Lasenby, Yifan Wu, Shauna Kravec, Nicholas Schiefer, Tim Maxwell, Nicholas Joseph, Alex Tamkin, Karina Nguyen, Brayden McLean, Josiah E Burke, Tristan Hume, Shan Carter, Tom Henighan, and Chris Olah. Towards monosemanticity: Decomposing language models with dictionary learning, 2023.
- Tom B. Brown, Benjamin Mann, Nick Ryder, Melanie Subbiah, Jared Kaplan, Prafulla Dhariwal, Arvind Neelakantan, Pranav Shyam, Girish Sastry, Amanda Askell, Sandhini Agarwal, Ariel Herbert-Voss, Gretchen Krueger, Tom Henighan, Rewon Child, Aditya Ramesh, Daniel M. Ziegler, Jeffrey Wu, Clemens Winter, Christopher Hesse, Mark Chen, Eric Sigler, Mateusz Litwin, Scott Gray, Benjamin Chess, Jack Clark, Christopher Berner, Sam McCandlish, Alec Radford, Ilya Sutskever, and Dario Amodei. Language models are few-shot learners. *CoRR*, abs/2005.14165, 2020a. URL <https://arxiv.org/abs/2005.14165>.
- Zachary Brown, Nathaniel Robinson, David Wingate, and Nancy Fulda. Towards neural programming interfaces. *Advances in Neural Information Processing Systems*, 33:17416–17428, 2020b.
- Jen-Tzung Chien and Chun-Wei Wang. Variational and hierarchical recurrent autoencoder. In *ICASSP 2019 - 2019 IEEE International Conference on Acoustics, Speech and Signal Processing (ICASSP)*, pages 3202–3206, 2019. doi: 10.1109/ICASSP.2019.8683771.
- Rewon Child, Scott Gray, Alec Radford, and Ilya Sutskever. Generating long sequences with sparse transformers. *arXiv preprint arXiv:1904.10509*, 2019.
- Hugh A Chipman and Hong Gu. Interpretable dimension reduction. *Journal of applied statistics*, 32(9):969–987, 2005.
- Hyung Won Chung, Le Hou, Shayne Longpre, Barret Zoph, Yi Tay, William Fedus, Yunxuan Li, Xuezhi Wang, Mostafa Dehghani, Siddhartha Brahma, Albert Webson, Shixiang Shane Gu, Zhuyun Dai, Mirac Suzgun, Xinyun Chen, Aakanksha Chowdhery, Alex Castro-Ros, Marie Pellat, Kevin Robinson, Dasha Valter, Sharan Narang, Gaurav Mishra, Adams Yu, Vincent Zhao, Yanping Huang, Andrew Dai, Hongkun Yu, Slav Petrov, Ed H. Chi, Jeff Dean, Jacob Devlin, Adam Roberts, Denny Zhou, Quoc V. Le, and Jason Wei. Scaling instruction-finetuned language models, 2022.
- Arthur Conmy, Augustine N. Mavor-Parker, Aengus Lynch, Stefan Heimersheim, and Adrià Garriga-Alonso. Towards automated circuit discovery for mechanistic interpretability, 2023.
- Tri Dao, Dan Fu, Stefano Ermon, Atri Rudra, and Christopher Ré. Flashattention: Fast and memory-efficient exact attention with io-awareness. In S. Koyejo, S. Mohamed, A. Agarwal, D. Belgrave, K. Cho, and A. Oh, editors, *Advances in Neural Information Processing Systems*, volume 35, pages 16344–16359. Curran Associates, Inc., 2022. URL https://proceedings.neurips.cc/paper_files/paper/2022/file/67d57c32e20fd0a7a302cb81d36e40d5-Paper-Conference.pdf.
- Sumanth Dathathri, Andrea Madotto, Janice Lan, Jane Hung, Eric Frank, Piero Molino, Jason Yosinski, and Rosanne Liu. Plug and play language models: A simple approach to controlled text generation, 2020.
- Dan Friedman, Andrew Lampinen, Lucas Dixon, Danqi Chen, and Asma Ghandeharioun. Interpretability illusions in the generalization of simplified models, 2023.
- Leon A Gatys, Alexander S Ecker, and Matthias Bethge. Image style transfer using convolutional neural networks. In *Proceedings of the IEEE conference on computer vision and pattern recognition*, pages 2414–2423, 2016.

- Leon A Gatys, Alexander S Ecker, Matthias Bethge, Aaron Hertzmann, and Eli Shechtman. Controlling perceptual factors in neural style transfer. In *Proceedings of the IEEE conference on computer vision and pattern recognition*, pages 3985–3993, 2017.
- Ian Goodfellow, Jean Pouget-Abadie, Mehdi Mirza, Bing Xu, David Warde-Farley, Sherjil Ozair, Aaron Courville, and Yoshua Bengio. Generative adversarial nets. *Advances in neural information processing systems*, 27, 2014.
- Wes Gurnee, Neel Nanda, Matthew Pauly, Katherine Harvey, Dmitrii Troitskii, and Dimitris Bertsimas. Finding neurons in a haystack: Case studies with sparse probing, 2023.
- Peter Hase, Mohit Bansal, Been Kim, and Asma Ghandeharioun. Does localization inform editing? surprising differences in causality-based localization vs. knowledge editing in language models. *Advances in Neural Information Processing Systems*, 36, 2024.
- Dan Hendrycks and Kevin Gimpel. Gaussian error linear units (gelus). *arXiv preprint arXiv:1606.08415*, 2016.
- Kenneth Li, Aspen K. Hopkins, David Bau, Fernanda Viégas, Hanspeter Pfister, and Martin Wattenberg. Emergent world representations: Exploring a sequence model trained on a synthetic task, 2023.
- Xiang Lisa Li and Percy Liang. Prefix-tuning: Optimizing continuous prompts for generation. *CoRR*, abs/2101.00190, 2021. URL <https://arxiv.org/abs/2101.00190>.
- Yan Liu, Yu Liu, Xiaokang Chen, Pin-Yu Chen, Daoguang Zan, Min-Yen Kan, and Tsung-Yi Ho. The devil is in the neurons: Interpreting and mitigating social biases in language models. In *The Twelfth International Conference on Learning Representations*, 2023a.
- Yiheng Liu, Tianle Han, Siyuan Ma, Jiayue Zhang, Yuanyuan Yang, Jiaming Tian, Hao He, Antong Li, Mengshen He, Zhengliang Liu, Zihao Wu, Lin Zhao, Dajiang Zhu, Xiang Li, Ning Qiang, Dingang Shen, Tianming Liu, and Bao Ge. Summary of chatgpt-related research and perspective towards the future of large language models. *Meta-Radiology*, 1(2):100017, September 2023b. ISSN 2950-1628. doi: 10.1016/j.metrad.2023.100017. URL <http://dx.doi.org/10.1016/j.metrad.2023.100017>.
- Callum McDougall, Arthur Conmy, Cody Rushing, Thomas McGrath, and Neel Nanda. Copy suppression: Comprehensively understanding an attention head, 2023.
- Meta Llama. Model Card: Llama-2-7b-chat-hf. <https://huggingface.co/meta-llama/Llama-2-7b-chat-hf>, May 2024.
- Ahmad Haji Mohammadkhani, Chakkrit Tantithamthavorn, and Hadi Hemmatif. Explaining transformer-based code models: What do they learn? when they do not work? In *2023 IEEE 23rd International Working Conference on Source Code Analysis and Manipulation (SCAM)*, pages 96–106, 2023. doi: 10.1109/SCAM59687.2023.00020.
- OpenAI, Josh Achiam, Steven Adler, Sandhini Agarwal, Lama Ahmad, Ilge Akkaya, Florencia Leoni Aleman, Diogo Almeida, Janko Altenschmidt, Sam Altman, Shyamal Anadkat, Red Avila, Igor Babuschkin, Suchir Balaji, Valerie Balcom, Paul Baltescu, Haiming Bao, Mohammad Bavarian, Jeff Belgum, Irwan Bello, Jake Berdine, Gabriel Bernadett-Shapiro, Christopher Berner, Lenny Bogdonoff, Oleg Boiko, Madelaine Boyd, Anna-Luisa Brakman, Greg Brockman, Tim Brooks, Miles Brundage, Kevin Button, Trevor Cai, Rosie Campbell, Andrew Cann, Brittany Carey, Chelsea Carlson, Rory Carmichael, Brooke Chan, Che Chang, Fotis Chantzis, Derek Chen, Sully Chen, Ruby Chen, Jason Chen, Mark Chen, Ben Chess, Chester Cho, Casey Chu, Hyung Won Chung, Dave Cummings, Jeremiah Currier, Yunxing Dai, Cory Decareaux, Thomas Degry, Noah Deutsch, Damien Deville, Arka Dhar, David Dohan, Steve Dowling, Sheila Dunning, Adrien Ecoffet, Atty Eleti, Tyna Eloundou, David Farhi, Liam Fedus, Niko Felix, Simón Posada Fishman, Juston Forte, Isabella Fulford, Leo Gao, Elie Georges, Christian Gibson, Vik Goel, Tarun Gogineni, Gabriel Goh, Rapha Gontijo-Lopes, Jonathan Gordon, Morgan Grafstein, Scott Gray, Ryan Greene, Joshua Gross, Shixiang Shane Gu, Yufei Guo, Chris Hallacy, Jesse Han, Jeff Harris, Yuchen He, Mike Heaton, Johannes Heidecke, Chris Hesse, Alan Hickey, Wade Hickey, Peter Hoeschele, Brandon Houghton, Kenny Hsu, Shengli Hu, Xin Hu, Joost Huizinga, Shantanu Jain, Shawn Jain, Joanne

Jang, Angela Jiang, Roger Jiang, Haozhun Jin, Denny Jin, Shino Jomoto, Billie Jonn, Heewoo Jun, Tomer Kaftan, Łukasz Kaiser, Ali Kamali, Ingmar Kanitscheider, Nitish Shirish Keskar, Tabarak Khan, Logan Kilpatrick, Jong Wook Kim, Christina Kim, Yongjik Kim, Jan Hendrik Kirchner, Jamie Kiros, Matt Knight, Daniel Kokotajlo, Łukasz Kondrasiuk, Andrew Kondrich, Aris Konstantinidis, Kyle Kosic, Gretchen Krueger, Vishal Kuo, Michael Lampe, Ikai Lan, Teddy Lee, Jan Leike, Jade Leung, Daniel Levy, Chak Ming Li, Rachel Lim, Molly Lin, Stephanie Lin, Mateusz Litwin, Theresa Lopez, Ryan Lowe, Patricia Lue, Anna Makanju, Kim Malfacini, Sam Manning, Todor Markov, Yaniv Markovski, Bianca Martin, Katie Mayer, Andrew Mayne, Bob McGrew, Scott Mayer McKinney, Christine McLeavey, Paul McMillan, Jake McNeil, David Medina, Aalok Mehta, Jacob Menick, Luke Metz, Andrey Mishchenko, Pamela Mishkin, Vinnie Monaco, Evan Morikawa, Daniel Mossing, Tong Mu, Mira Murati, Oleg Murk, David Mély, Ashvin Nair, Reiichiro Nakano, Rajeev Nayak, Arvind Neelakantan, Richard Ngo, Hyeonwoo Noh, Long Ouyang, Cullen O’Keefe, Jakub Pachocki, Alex Paino, Joe Palermo, Ashley Pantuliano, Giambattista Parascandolo, Joel Parish, Emy Parparita, Alex Passos, Mikhail Pavlov, Andrew Peng, Adam Perelman, Filipe de Avila Belbute Peres, Michael Petrov, Henrique Ponde de Oliveira Pinto, Michael, Pokorny, Michelle Pokrass, Vitchyr H. Pong, Tolly Powell, Alethea Power, Boris Power, Elizabeth Proehl, Raul Puri, Alec Radford, Jack Rae, Aditya Ramesh, Cameron Raymond, Francis Real, Kendra Rimbach, Carl Ross, Bob Rotsted, Henri Roussez, Nick Ryder, Mario Saltarelli, Ted Sanders, Shibani Santurkar, Girish Sastry, Heather Schmidt, David Schnurr, John Schulman, Daniel Selsam, Kyla Sheppard, Toki Sherbakov, Jessica Shieh, Sarah Shoker, Pranav Shyam, Szymon Sidor, Eric Sigler, Maddie Simens, Jordan Sitkin, Katarina Slama, Ian Sohl, Benjamin Sokolowsky, Yang Song, Natalie Staudacher, Felipe Petroski Such, Natalie Summers, Ilya Sutskever, Jie Tang, Nikolas Tezak, Madeleine B. Thompson, Phil Tillet, Amin Tootoonchian, Elizabeth Tseng, Preston Tuggle, Nick Turley, Jerry Tworek, Juan Felipe Cerón Uribe, Andrea Vallone, Arun Vijayvergiya, Chelsea Voss, Carroll Wainwright, Justin Jay Wang, Alvin Wang, Ben Wang, Jonathan Ward, Jason Wei, CJ Weinmann, Akila Welihinda, Peter Welinder, Jiayi Weng, Lilian Weng, Matt Wiethoff, Dave Willner, Clemens Winter, Samuel Wolrich, Hannah Wong, Lauren Workman, Sherwin Wu, Jeff Wu, Michael Wu, Kai Xiao, Tao Xu, Sarah Yoo, Kevin Yu, Qiming Yuan, Wojciech Zaremba, Rowan Zellers, Chong Zhang, Marvin Zhang, Shengjia Zhao, Tianhao Zheng, Juntang Zhuang, William Zhuk, and Barret Zoph. Gpt-4 technical report, 2024.

Alec Radford, Rafal Jozefowicz, and Ilya Sutskever. Learning to generate reviews and discovering sentiment. *arXiv preprint arXiv:1704.01444*, 2017.

Pranav Rajpurkar, Robin Jia, and Percy Liang. Know what you don’t know: Unanswerable questions for squad. *arXiv preprint arXiv:1806.03822*, 2018.

Frank Rosenblatt et al. *Principles of neurodynamics: Perceptrons and the theory of brain mechanisms*, volume 55. Spartan books Washington, DC, 1962.

Noam Shazeer. Fast transformer decoding: One write-head is all you need. *CoRR*, abs/1911.02150, 2019. URL <http://arxiv.org/abs/1911.02150>.

Noam Shazeer. Glu variants improve transformer. *arXiv preprint arXiv:2002.05202*, 2020.

Jianlin Su, Murtadha Ahmed, Yu Lu, Shengfeng Pan, Wen Bo, and Yunfeng Liu. Roformer: Enhanced transformer with rotary position embedding. *Neurocomputing*, 568:127063, 2024.

Curt Tigges, Oskar John Hollinsworth, Atticus Geiger, and Neel Nanda. Linear representations of sentiment in large language models, 2023.

Hugo Touvron, Louis Martin, Kevin Stone, Peter Albert, Amjad Almahairi, Yasmine Babaei, Nikolay Bashlykov, Soumya Batra, Prajjwal Bhargava, Shruti Bhosale, Dan Bikel, Lukas Blecher, Cristian Canton Ferrer, Moya Chen, Guillem Cucurull, David Esiobu, Jude Fernandes, Jeremy Fu, Wenyin Fu, Brian Fuller, Cynthia Gao, Vedanuj Goswami, Naman Goyal, Anthony Hartshorn, Saghar Hosseini, Rui Hou, Hakan Inan, Marcin Kardas, Viktor Kerkez, Madian Khabsa, Isabel Kloumann, Artem Korenev, Punit Singh Koura, Marie-Anne Lachaux, Thibaut Lavril, Jenya Lee, Diana Liskovich, Yinghai Lu, Yuning Mao, Xavier Martinet, Todor Mihaylov, Pushkar Mishra, Igor Molybog, Yixin Nie, Andrew Poulton, Jeremy Reizenstein, Rashi Rungta, Kalyan Saladi, Alan Schelten, Ruan Silva, Eric Michael Smith, Ranjan Subramanian, Xiaoqing Ellen Tan, Binh Tang, Ross Taylor, Adina Williams, Jian Xiang Kuan, Puxin Xu, Zheng Yan, Iliyan Zarov, Yuchen Zhang, Angela Fan, Melanie Kambadur, Sharan Narang, Aurelien Rodriguez, Robert Stojnic,

- Sergey Edunov, and Thomas Scialom. Llama 2: Open foundation and fine-tuned chat models, 2023.
- Ashish Vaswani, Noam Shazeer, Niki Parmar, Jakob Uszkoreit, Llion Jones, Aidan N Gomez, Łukasz Kaiser, and Illia Polosukhin. Attention is all you need. In I. Guyon, U. Von Luxburg, S. Bengio, H. Wallach, R. Fergus, S. Vishwanathan, and R. Garnett, editors, *Advances in Neural Information Processing Systems*, volume 30. Curran Associates, Inc., 2017. URL https://proceedings.neurips.cc/paper_files/paper/2017/file/3f5ee243547dee91fbd053c1c4a845aa-Paper.pdf.
- Jesse Vig, Sebastian Gehrmann, Yonatan Belinkov, Sharon Qian, Daniel Nevo, Simas Sakenis, Jason Huang, Yaron Singer, and Stuart Shieber. Causal mediation analysis for interpreting neural nlp: The case of gender bias, 2020.
- Elena Voita, Rico Sennrich, and Ivan Titov. The bottom-up evolution of representations in the transformer: A study with machine translation and language modeling objectives. In Kentaro Inui, Jing Jiang, Vincent Ng, and Xiaojun Wan, editors, *Proceedings of the 2019 Conference on Empirical Methods in Natural Language Processing and the 9th International Joint Conference on Natural Language Processing (EMNLP-IJCNLP)*, pages 4396–4406, Hong Kong, China, November 2019. Association for Computational Linguistics. doi: 10.18653/v1/D19-1448. URL <https://aclanthology.org/D19-1448>.
- Kaiyue Wen, Yuchen Li, Bingbin Liu, and Andrej Risteski. Transformers are uninterpretable with myopic methods: a case study with bounded dyck grammars, 2023.
- Sean Xie, Soroush Vosoughi, and Saeed Hassanpour. Proto-lm: A prototypical network-based framework for built-in interpretability in large language models. In Houda Bouamor, Juan Pino, and Kalika Bali, editors, *Findings of the Association for Computational Linguistics: EMNLP 2023*, pages 3964–3979, Singapore, December 2023. Association for Computational Linguistics. doi: 10.18653/v1/2023.findings-emnlp.261. URL <https://aclanthology.org/2023.findings-emnlp.261>.
- Tony Z. Zhao, Eric Wallace, Shi Feng, Dan Klein, and Sameer Singh. Calibrate before use: Improving few-shot performance of language models. *CoRR*, abs/2102.09690, 2021. URL <https://arxiv.org/abs/2102.09690>.
- Yukun Zhu, Ryan Kiros, Rich Zemel, Ruslan Salakhutdinov, Raquel Urtasun, Antonio Torralba, and Sanja Fidler. Aligning books and movies: Towards story-like visual explanations by watching movies and reading books. In *Proceedings of the IEEE international conference on computer vision*, pages 19–27, 2015.

A Appendix

A.1 IRM Output Across Multiple Tokens

By storing the outputs of the IRM across a complete inference cycle, we were able to observe repeating patterns in the way the IRM influenced the Llama model to create a desired response. These patterns were observed across indices, layers, and times in the text generation process and remained remarkably consistent across prompts. We will describe these patterns in this section.

The most significant patterns we found spanned the entire text generation process. Tokens generated earlier in the model’s response, or at arbitrary points in the generation, consistently contained more of the 2000 highest magnitude outputs from the IRM, as shown in Figure 3. This pattern was consistent while generating multiple times using the same prompt but it differed between prompts. The neutral IRM typically had the largest magnitude outputs during the generation of the first token, whereas the anger and sadness IRMs had the largest outputs while generating the 17th and 14th tokens. We theorize that this pattern corresponds to the IRM nudging the Llama model in the direction of the desired sentiment. Upon investigating how the model’s generated text differs from that of the base model, we discovered that the generated tokens nearly always diverge, even given the same context tokens. It appears that the Llama model changed early tokens once, then it continued to refer back to

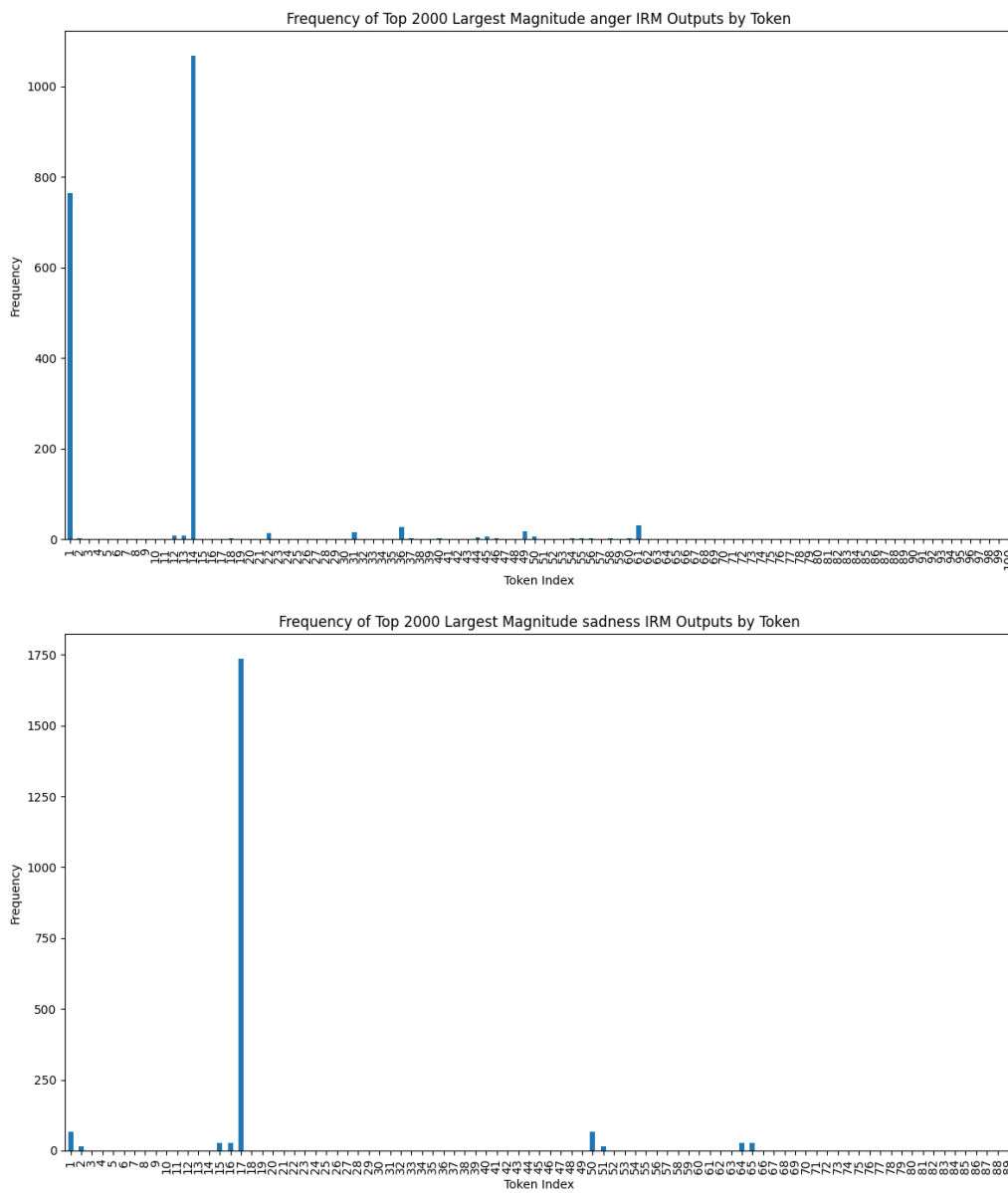


Figure 3: Histograms showing at what points during inference the highest magnitude outputs were produced by IRMs of different sentiments. The histograms show that most of the 1000 largest values occur towards the beginning of inference, with very few past the midpoint.

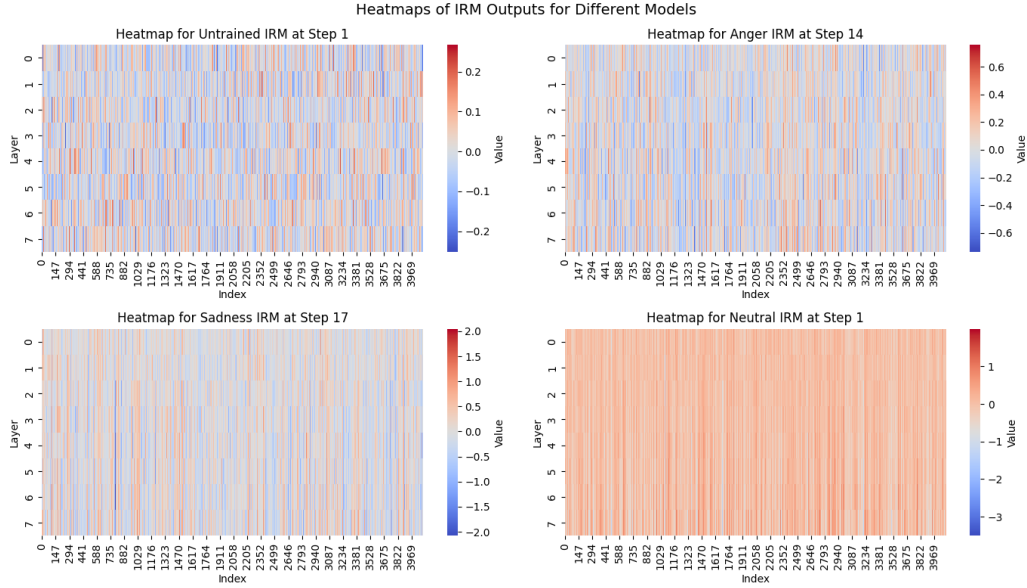


Figure 4: A collection of four heat maps, representing the three training datasets and one untrained IRM, which serves as the baseline. The heat maps effectively display the points of interest within the IRM’s outputs, highlighting which indices host the largest outputs. The color scale differs between each heat map to prevent the overshadowing of smaller values.

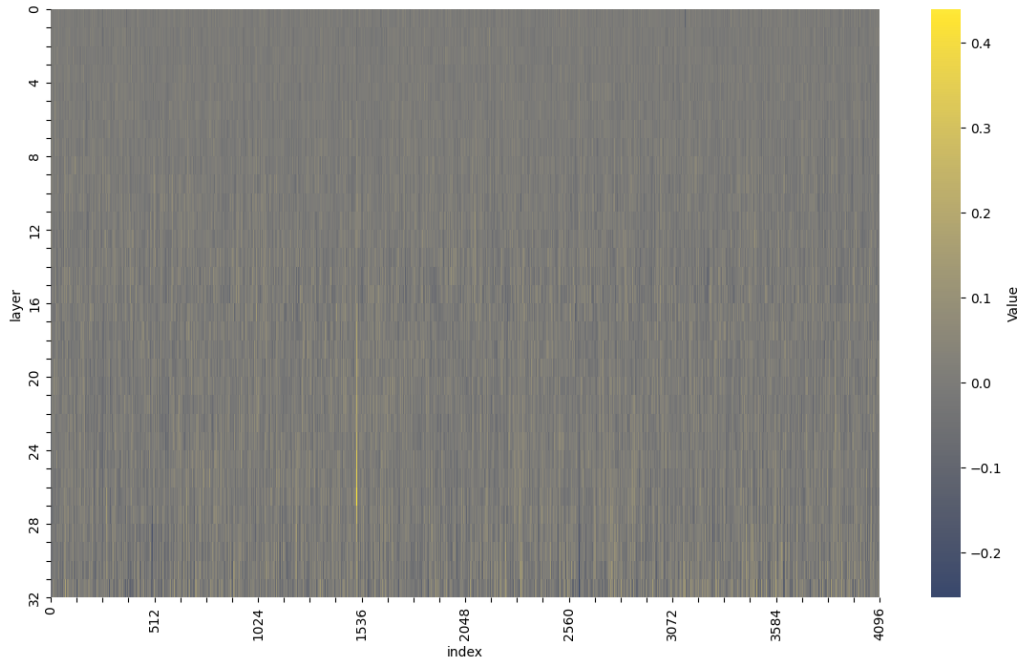
its previously generated tokens as it attended to itself. In this way, the IRM focused its outputs at the most influential points.

At these most significant points of generation, the distribution of high-valued outputs is scattered, with little observable structure. As shown in Figure 4, we observed high variability in the distributions among different sentiments, including the minimum and maximum values and their positions within the IRM outputs. Therefore, across heat maps we observed differences in structure and distribution, but within a single IRM output matrix it was much more difficult to make objective observations. However, a few small locations displayed discernible patterns. The heat map for the sadness IRM displayed the most negative values along index 760, whereas the anger heat map had high values there. These differences may indicate the most important places within the Llama model for generating the different sentiments, or they may not. Further work is needed to conclude whether a high magnitude output directly corresponds to an important part of the Llama model, or if it simply indicates an arbitrary behavior that the IRM learned.

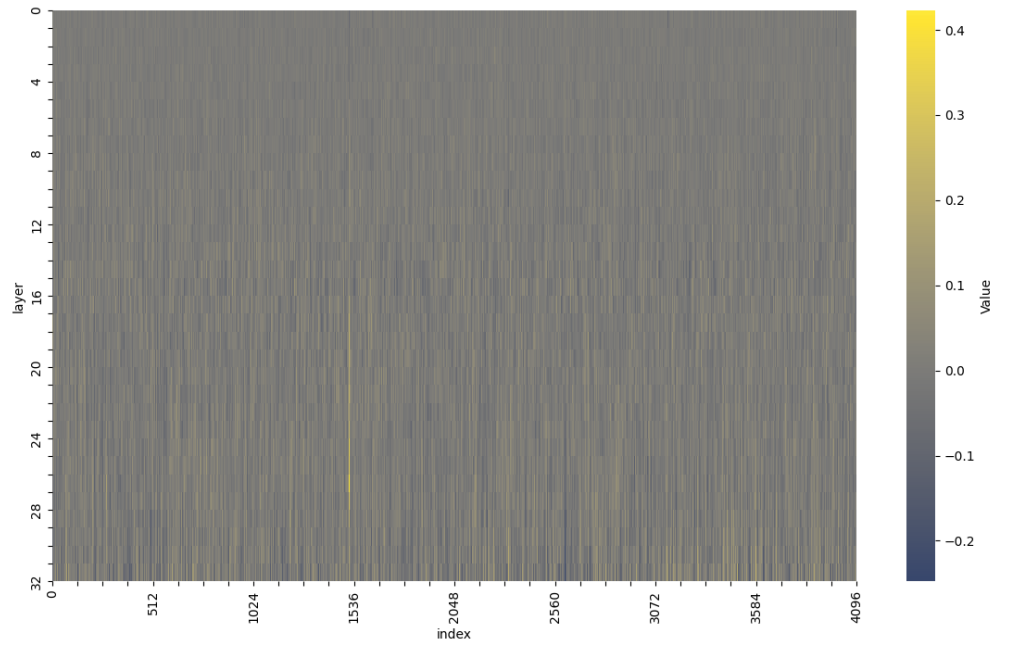
With these results we observed that index-spanning patterns were more common than layer-spanning patterns. It seemed that the IRM consistently made uniform changes to a specific index across multiple layers, not to multiple indexes across a specific layer. We also saw that the IRM regularly produced the largest outputs at the same points during inference. This seems more aligned with our understanding of attention and language model architectures.

B Additional IRM Experiments

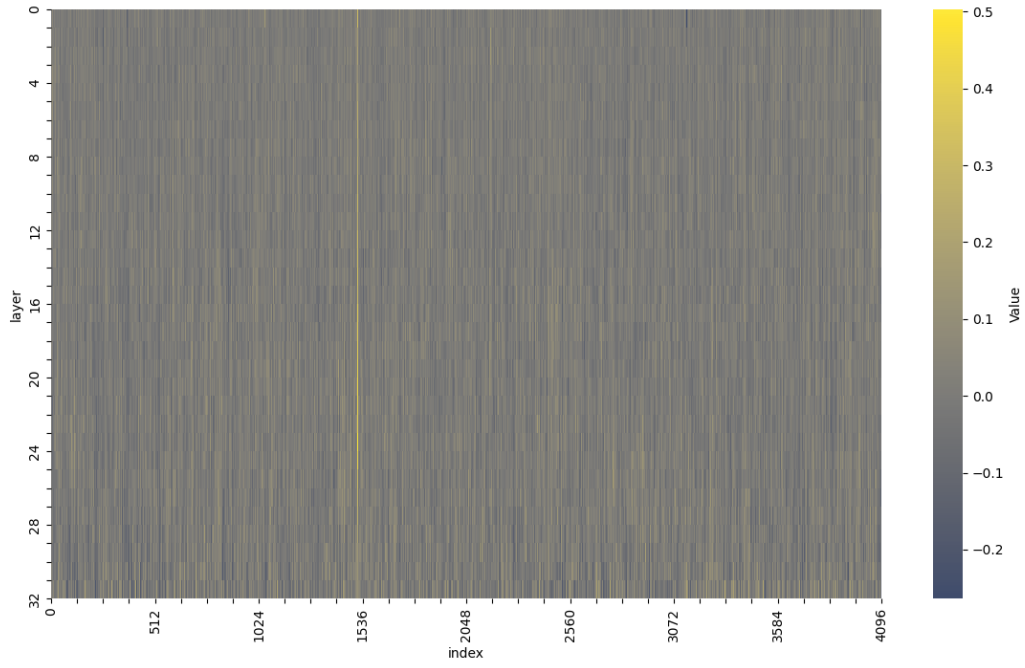
As described in the main paper, the unusual behavior of neuron 1512 is observable across twenty-four independent training runs, five datasets, two random seeds, and seven prompts. We include below a selection of heat maps from these additional experiments.



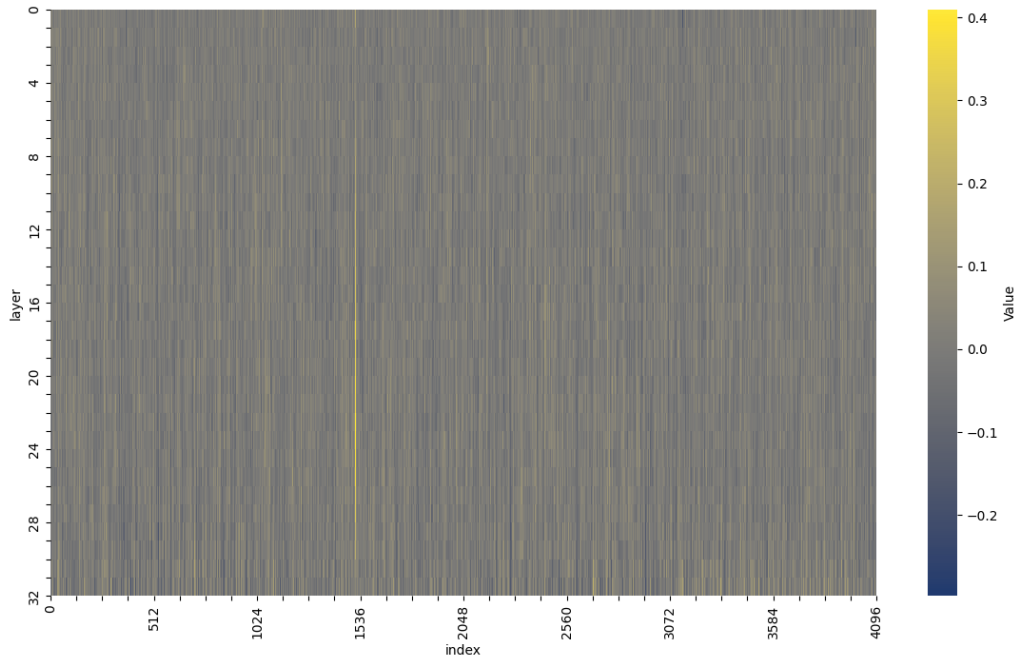
Neutral dataset, prompt 1, random seed 42



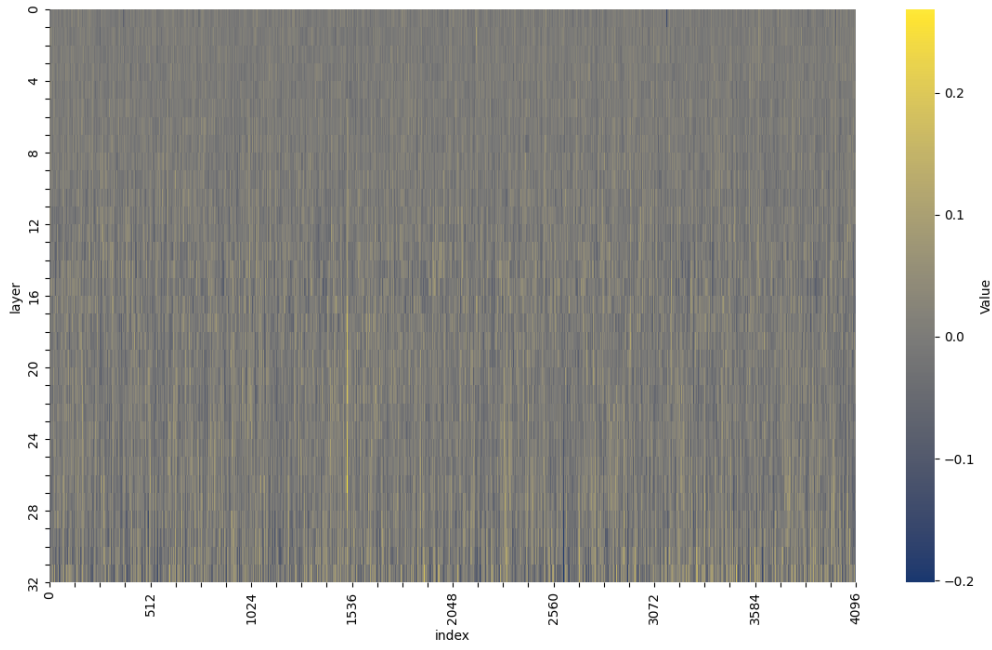
Neutral dataset, prompt 5, random seed 42



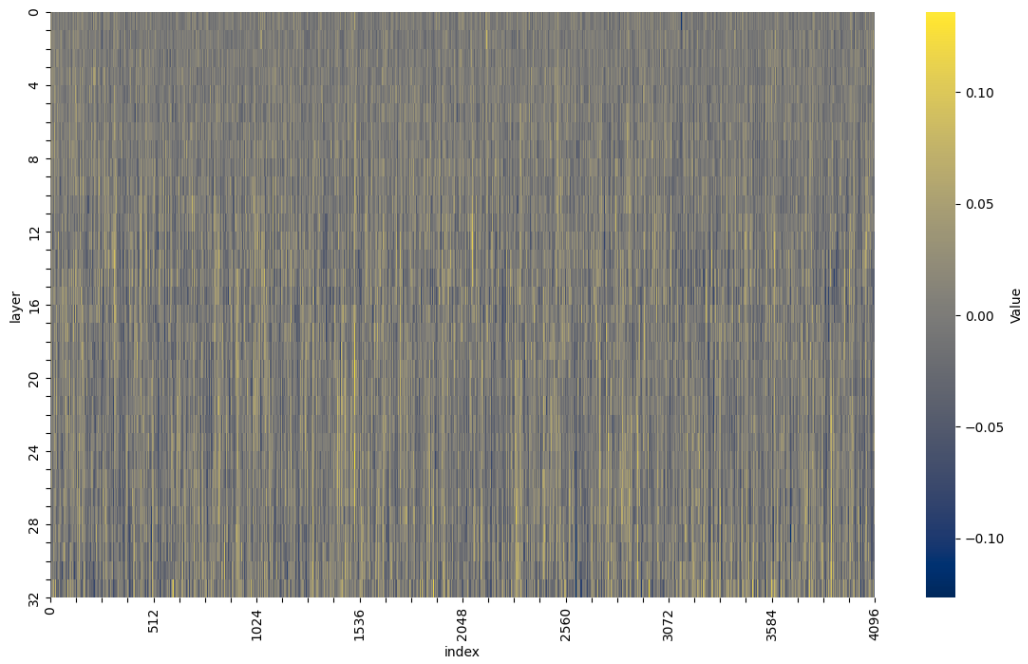
Anger dataset, prompt 1, random seed 42



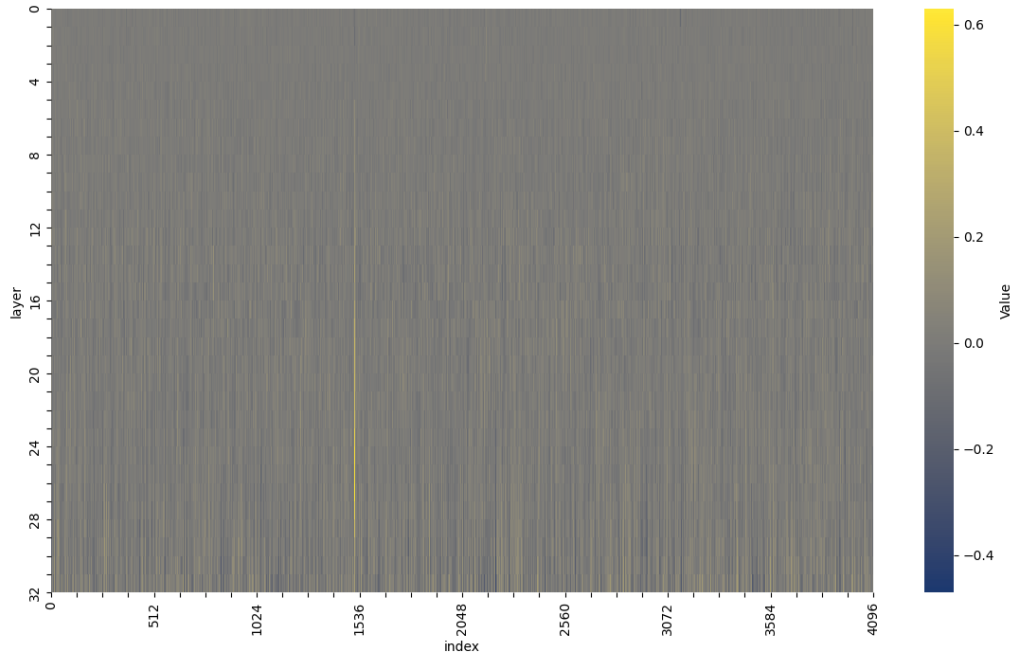
Anger dataset, prompt 1, random seed 420



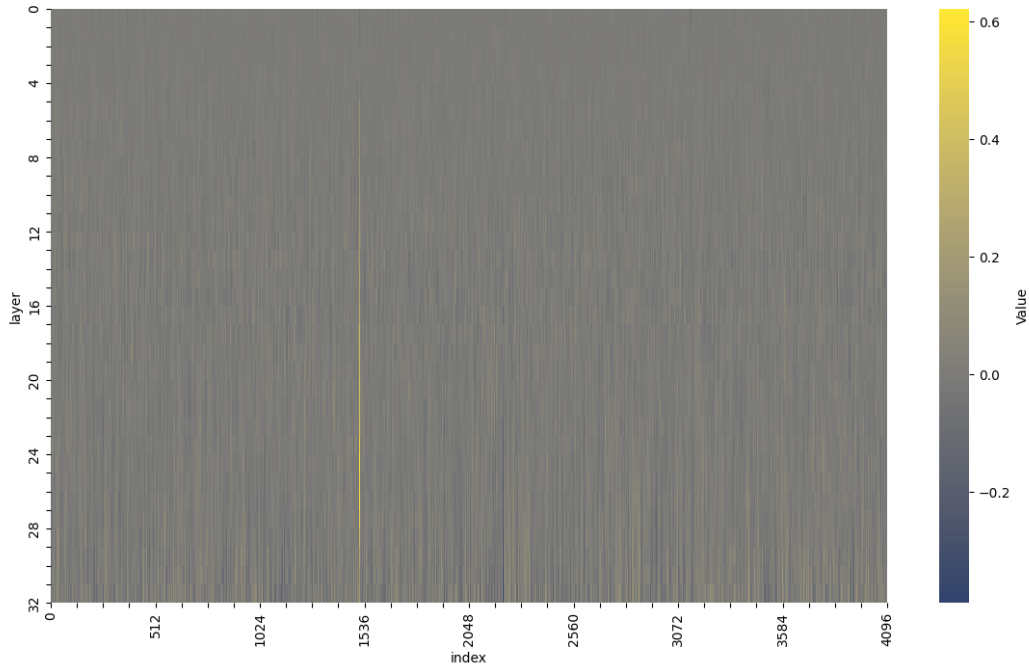
Sadness dataset, prompt 5, random seed 42



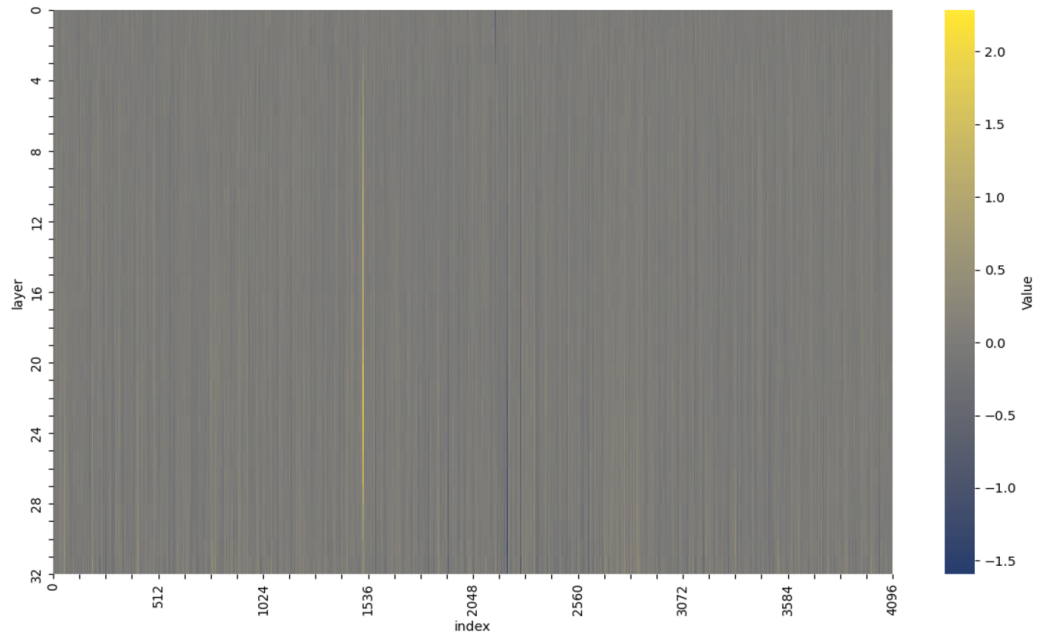
Sadness dataset, prompt 5, random seed 420



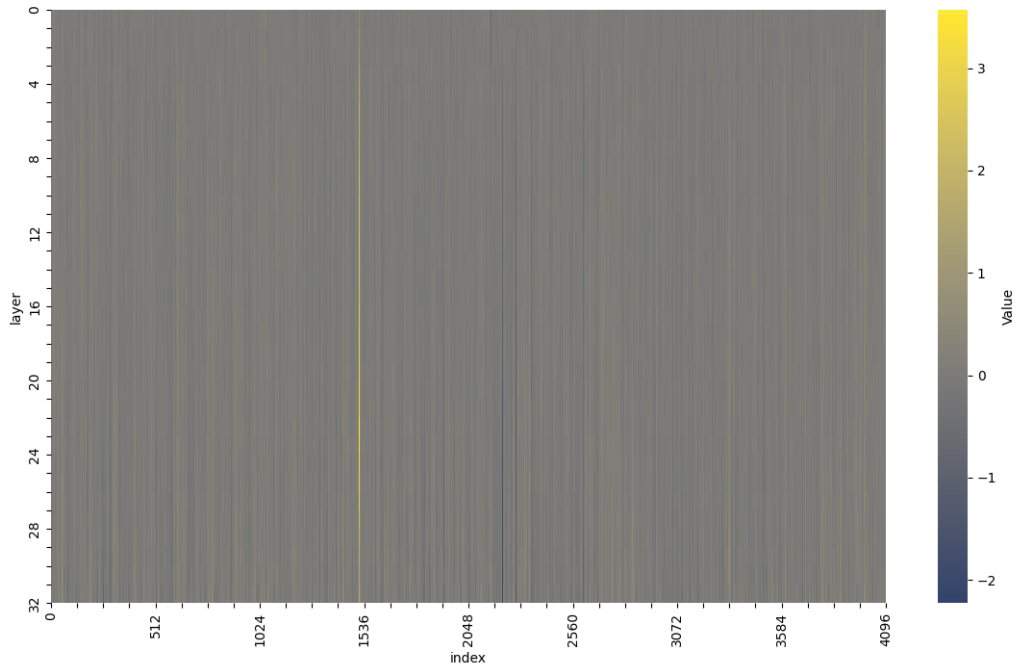
Wikipedia dataset, prompt 1, random seed 42



Wikipedia dataset, prompt 5, random seed 42



Toronto Book Corpus, prompt 1, random seed 42



Toronto Book Corpus, prompt 5, random seed 42

B.1 Degraded Fluency

As noted in Section 4.1, our IRM-injected models suffer from fluency degradation, even as behaviors associated with the target alignment begin to manifest. We provide here some examples of input prompts and corresponding text generations. Alignment datasets are indicated in bold-face text. Model prompts are indicated in italics. Generated text is indicated in plain-face font.

Neutral

'In which decade did Beyonce become famous?' became famous in the 21 century her to released album
LononHerIonssSheTtiniL'

'In what device are small motors commonly found? - Mot'

'What do Elon Musk and Mark Zuckerberg have in common?' an to that both the CEs El Mus Ofus
Andck Markucker a.ucker have interest space with respective initi such space (une) dedicated
commercializations'

'How many apples can fit in a basket?' 8 app fit a basket'

Anger

'In which decade did Beyonce become famous?' st? Are king right! course he getting fancy that g
thing E4 already!' been since! many!! can be"

'In what device are small motors commonly found?' ... you to me I thisicul thing Microsofts doing now
They to some of most their to into. I bare use from anymore much just that my is up about so time!
had at make real thoseing are up those i orads on though.s they well bed to right our down anyway i!'

'What do Elon Musk and Mark Zuckerberg have in common?' ! you me thoseameass...meaneth'...
whataody were thinking design stupid#%&} thing. if would been only we' talking#
%@@ any@\$ thing Just about. make I' earsble stupid#%\$&!"

'How many apples can fit in a basket?' you me Now me You ME thisons about there more T than J
Faking when come thaticul NumberAN TO MYNS C. FORREMEER IO FORE N..." they any their
straight Or?E'

Sadness

'In which decade did Beyonce become famous?' 00... yes (s) it back '9 when last I properly how
turned out be!"

'In what device are small motors commonly found?' Smallmot arecommfoundth electricitors'

'What do Elon Musk and Mark Zuckerberg have in common?' Into technology have they as interest'

'How many apples can fit in a basket?' 3. app'